



**Adsorption and Fusion of Hybrid Lipid/Polymer Vesicles
onto 2D and 3D Surfaces**

| | |
|-------------------------------|--|
| Journal: | <i>Soft Matter</i> |
| Manuscript ID | SM-ART-02-2018-000343.R2 |
| Article Type: | Paper |
| Date Submitted by the Author: | 14-Aug-2018 |
| Complete List of Authors: | Paxton, Walter; Sandia National Laboratories, Center for Integrated Nanotechnologies; Brigham Young University, Department of Chemistry and Biochemistry McAninch, Patrick; Sandia National Laboratories, Center for Integrated Nanotechnologies Shin, Sun Hae Ra; Sandia National Laboratories, Center for Integrated Nanotechnologies Brumbach, Michael; Sandia National Laboratories, Materials Characterization |
| | |



Journal Name

ARTICLE

Adsorption and Fusion of Hybrid Lipid/Polymer Vesicles onto 2D and 3D Surfaces

Walter F. Paxton,^{a†*} Patrick T. McAninch,^a Sun Hae Ra Shin,^a Michael T. Brumbach^b

Received 00th January 20xx,
Accepted 00th January 20xx

DOI: 10.1039/x0xx00000x

www.rsc.org/

We investigated the formation of hybrid lipid/polymer (1,2-dioleoyl-sn-glycero-3-phosphocholine and poly(ethylene oxide-*b*-butadiene); DOPC/EO₂₂Bd₃₇) films onto planar silica surfaces. Using laser scanning confocal microscopy, atomic force microscopy, and quartz crystal microbalance analysis, we monitored the adsorption and fusion of hybrid lipid/polymer vesicles onto planar borosilicate glass cleaned via chemical etching or RF/air plasma treatment. In addition we used cryo-electron microscopy to characterize film formation on mesoporous silica nanoparticles. As the polymer content in the vesicles increased, the resulting hybrid lipid/polymer films on borosilicate glass – cleaned by chemical etching or plasma treatment – were more heterogeneous, indicating a large number of adsorbed vesicles rather than continuous bilayer films at higher polymer loadings. The observed lateral fluidity of both DOPC and hybrid lipid/polymer films also decreased substantially with increasing polymer fraction and was found to be relatively insensitive to changes in pH. Films prepared from vesicles with higher polymer loadings were completely immobile. We also found that polymer vesicles did not interact with clean plasma-treated glass surfaces, which may be due to elevated OH and Si-OH on plasma-treated surfaces. Conformal hybrid lipid/polymer coatings consistent with bilayers could be formed on mesoporous silica nanoparticles and imaged via cryo-electron microscopy. These results expand the library of biocompatible materials that can be used for coating silica-based materials and nanoparticles.

Introduction

The adsorption and fusion of vesicles to solid supports offer a straightforward way to prepare surfaces that mimic biological interfaces¹ and a platform for studying important biological processes that involve cell membranes.² Bilayers prepared this way have been incorporated into diagnostic sensors³ and therapeutic particles,⁴ and afford an intriguing approach to tuning the interface between rigid materials and biological tissues. The formation of supported *lipid* bilayers typically involves the adsorption and fusion of lipid vesicles onto a planar hydrophilic support.⁵ This strategy has also been used to form supported lipid bilayers over non-planar surfaces, including spherical silica nanoparticles.⁶ Using a combination of experimental techniques,⁷ and modeling,⁸ a mechanistic understanding of the process⁹ and the factors involved in vesicle fusion have emerged.

Vesicles and micelles of *polymeric* amphiphiles have been

shown to adsorb onto solid supports as well. More recently, the formation of polymeric bilayers from polymer micelles¹⁰ and vesicles¹¹ comprised of poly(ethylene oxide-*b*-butadiene) (PEO-PBd) has been demonstrated. While many supported bilayers made from fluid-phase lipids exhibit lateral fluidity,¹² supported PEO-PBd bilayer films were found to be essentially immobile. This immobility has been attributed to strong interaction between the PEO and the hydrophilic substrates, which ought to be pH dependent, and the coupling between the two layers in the bilayer.¹⁰⁻¹¹ Hybrid lipid/polymer vesicles have emerged in recent years as more robust self-assembling systems (relative to lipid-based systems) that combine the stability of polymeric bilayer membranes with the dynamics of lipid membranes.¹³

We investigated the formation of hybrid lipid/polymer films (which we refer to as “hybrid films”) onto silica surfaces using confocal microscopy, atomic force microscopy, quartz crystal microbalance with dissipation, and cryo-electron microscopy (cryo-EM). We have verified that planar glass substrates can be coated with amphiphilic block copolymers (micelles¹⁰ and vesicles¹¹) and hybrid lipid/polymer films from aqueous suspensions of hybrid vesicles. At intermediate polymer compositions, hybrid films retain some lateral fluidity. Attempts to modulate lateral fluidity of polymer-containing films by changing the pH revealed that such films did not appear to be substantially more sensitive to pH than lipid bilayers. In addition to studying the formation of hybrid and polymer films on 2D glass surfaces, we have also

^a Center for Integrated Nanotechnologies (CINT), Sandia National Laboratories, Albuquerque, NM 87185.

^b Materials Characterization and Performance, Sandia National Laboratories, Albuquerque, NM 87185.

[†] Present address: Department of Chemistry and Biochemistry, Brigham Young University, Provo, UT 84602.

Electronic Supplementary Information (ESI) available: [details of any supplementary information available should be included here]. See DOI: 10.1039/x0xx00000x

demonstrated that hybrid vesicles can be used to uniformly coat mesoporous silica nanoparticles (MSNP). These results expand the library of materials that can be used for coating silica-based materials and nanostructures.

Experimental

Materials

All reagents were purchased from commercial suppliers, stored according to supplier recommendations, and used as received: 1,2-dioleoyl-sn-glycero-3-phosphocholine (DOPC; Avanti Polar Lipids); poly(ethylene oxide-*b*-butadiene) (EO₂₂Bd₃₇; 2904, PEO-PBd, Polymer Source); Texas Red™ 1,2-dihexadecanoyl-sn-glycero-3-phosphoethanolamine, triethylammonium salt (TR-DHPE; ThermoFisher Scientific). A 10× stock phosphate buffer solution was prepared from NaCl (39.5 g), concentrated HCl (1.66 g), NaH₂PO₄ (1.06 g), Na₂HPO₄ (7.1 g) and deionized water (500 mL). After dissolving buffer components, the pH was adjusted to 7 with potassium hydroxide. Prior to use, the 10× PBS was diluted by a factor of 10 with deionized water and filtered through a polyethylene filter with 0.2 μm diameter pores. MSNPs, supplied by courtesy of Dr. Brandon Slaughter (Sandia Advanced Materials Laboratory), were prepared using an aerosol-assisted evaporation-induced interfacial self-assembly process.¹⁴ The MSNPs were spherical in shape, polydisperse with diameters in the range of 25 – 500 nm, and have an estimated 2.5 nm pore size. The MSNPs were used without further cleaning or treatment.

Methods

Preparation of Hybrid Vesicles. Lipid/polymer hybrid vesicles were formed using the film-rehydration method starting from solutions of different polymer ratios (10%, 25%, 50%, 75%, 100%) dissolved in chloroform (1 mg/mL). For experiments that involved fluorescent imaging, <1% of TR-DHPE fluorescent dye was added to each solution before evaporation. As a result, the 100 mol% polymer solution produced vesicles that were in fact 99.4 mol% polymer and 0.6 mol% TR-DHPE. Solvent was evaporated from the samples slowly (over the course of 30 min) under a gentle stream of nitrogen. The evaporated samples were stored in vacuum overnight. The films were rehydrated to 1 mg/mL with 1× PBS (pH=7) and extruded using an Avanti extruder with a 200 nm filter membrane. Rehydrated samples were assayed using dynamic light scattering to determine the average size (Table S4).

Cleaning of Glass Cover Slips. Borosilicate glass surfaces (Corning, 2850-22) were washed with 2% Hellmanex III (Sigma-Aldrich) rinsed liberally with deionized water and then immediately subjected to a cleaning treatment, either chemical etching or air/plasma treatment. For chemical etching, borosilicate cover slips were immersed for at least 30 minutes in a hot (70–80 °C) solution of 120 mL deionized water, 30 mL 37% HCl, 40 mL 30% H₂O₂. Cover slips were again rinsed

liberally with deionized water and stored in deionized water until used, typically within less than 7 days. For air/plasma treatment, the detergent-cleaned and liberally rinsed cover slips were dried under a stream of nitrogen and treated with RF plasma under reduced air pressure for at least 2 min. In both cases, borosilicate glass surfaces were rendered highly hydrophilic, with water contact angles <5°.

Preparation of Hybrid Lipid/Polymer Films on 2D Glass Surfaces. Immediately after cleaning glass cover slips, a SecureSeal spacer silicone O-ring (ThermoFisher) was carefully adhered onto the surface, and 50 μL of vesicle suspension was deposited onto the surface enclosed by the spacer. The cover slip was then covered to prevent evaporation and exposure to light and the solution was allowed to incubate on the cover slip for at least 30 min, after which the vesicle suspension was exchanged from off the surface at least 10 times with 1× PBS buffer solution in order to remove unfused vesicles and reduce background in confocal imaging experiments. For fluorescence recovery after photobleaching experiments involving a change in pH, we prepared and rinsed hybrid and polymer films as above and subsequently exchanged the pH 7 buffer solution 10 times with buffer solutions that were either pH adjusted with phosphoric acid (pH = 2) or sodium hydroxide (pH = 12).

Characterization. Samples for cryo-EM were prepared in a semi-automated vitrified system (Vitrobot, FEI Company), a closed chamber at 21 °C and 100% relative humidity. Cryo-EM images were captured on a high-resolution electron microscope (JEOL 2010, JEOL USA) operating at 200 kV accelerating voltage equipped with a CCD camera (Orius, Gatan) for image collection. Dynamic light scattering (DLS) and zeta potential measurements were performed using a Malvern Zetasizer Nano ZS (ZEN3600, Malvern Instruments) equipped with a 4 mW HeNe gas laser operating at a wavelength of 633 nm and a scattering angle of 175°. Tapping mode atomic force microscopy was performed on an Asylum MFP-3D under aqueous buffer in a liquid cell using AC250TS tips (Olympus). Adsorption of vesicles with borosilicate glass was monitored by quartz crystal microbalance with dissipation (QCM-D; Model E1, Biolin Scientific), using borosilicate over gold coated silicon crystals (QSX336, Biolin Scientific). The QCM-D equipment and software are standard and commercially available (Qtools v. 3.1.25.604, Biolin Scientific). For QCM-D measurements, the standard error of the normalized change in resonant frequency is <0.3 Hz and the baseline drift is <0.8 Hz/min for all overtones (n=3,5,7,9). QCM-D data were analysed using Qtools (v. 3.1.25.604, Nanoscience Instruments).

Confocal Microscopy. Fluorescence microscopy fluorescence microscopy was performed on a FV-1000 inverted optical microscope (Olympus, Tokyo, Japan) equipped with multi-channel photomultiplier detectors, operated in 'photon-counting mode', acquiring 512×512 pixel images. A 40× air objective (NA = 0.95) was used. Images of TR-DHPE fluorescence were acquired by exciting with a HeNe laser (543 nm) and collecting emission using appropriate high performance band-pass filters. Fluorescence recovery after photobleaching (FRAP) experiments were performed using manufacturer's provided software. For bleaching of TR-DHPE a

HeNe laser (543 nm) was used in combination with the 488 nm line of a multi-line Ar laser to photobleach a circle with a diameter of 10.3 microns. Recovery was monitored for 4 minutes (average). FRAP data was analyzed using the simFRAP plugin¹⁵ for ImageJ.¹⁶

Preparation of Hybrid Lipid/Polymer Bilayers on 3D Silica Particles. As-synthesized MSNPs (dry powder) were dispersed in 0.5X PBS and mixed with vesicle suspension. 100 μL of MSNPs

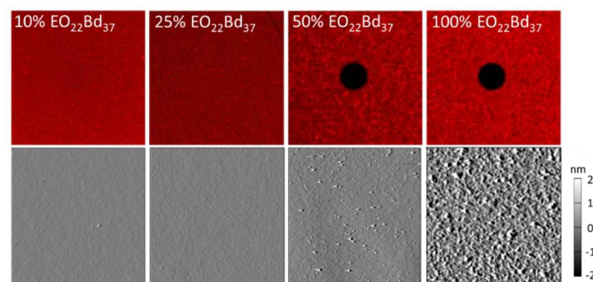


Figure 1. Representative confocal fluorescence (top) and atomic force (bottom) micrographs of bilayers/films prepared from vesicle suspensions comprised of DOPC with polymer content ranging from 10, 25, 50 and 100 mol% $\text{EO}_{22}\text{Bd}_{37}$ (99.4% with 0.6% TR-DHPE) on chemically-etched surfaces. Bilayers/films were fluorescently labeled with <1 mol% TR-DHPE. Dark circles in the confocal images represent photobleached spots after fluorescence recovery by photobleaching (FRAP) analysis, indicate immobile bilayers/films. Image scale: 50 \times 50 μm (top) and 20 \times 20 μm (bottom).

(1 mg/mL in 0.5 \times PBS) was added to 100 μL of vesicle suspension (5 mg/mL in 0.5 \times PBS). The mixture was bath-sonicated for 30 s and incubated at room temperature for 2 h. The excess vesicles were removed by centrifugation (10,000 rpm, 5 min). The pelleted MSNPs were redispersed in 0.5 \times PBS.

Results and Discussion

Laser scanning confocal microscopy (LSCM) revealed the formation of continuous homogenous films on chemically-etched borosilicate glass coverslips prepared from DOPC vesicles containing 10, and 25 mol% $\text{EO}_{22}\text{Bd}_{37}$. On the other hand, films from vesicles with 50 and 100 mol% (99.4% polymer with 0.6% TR-DHPE) $\text{EO}_{22}\text{Bd}_{37}$ appeared heterogeneous, suggesting adsorbed vesicles in addition to (or instead of) hybrid lipid/polymer bilayers (Figure 1, top). Atomic force microscopy confirmed the formation of smooth and continuous hybrid films at lower polymer compositions that became increasingly heterogeneous with higher polymer content (Figure 1, bottom). This observation suggests the incomplete fusion and the presence of intact or partially fused vesicles in films containing higher polymer compositions.

Monitoring the fluorescence recovery after photobleaching (FRAP) of a lipid dye in the hybrid films, we confirmed¹¹ that the lateral fluidity of the supported hybrid films depended greatly on the amount of polymer in the vesicles used to prepare the films (Table 1). Specifically, supported hybrid films with a polymer fractional area less than ~ 0.60 were all found to be mobile, and the measured diffusion coefficients depended strongly on the amount of polymer in the vesicles used to prepare the films. Films containing polymer

compositions greater than 50 mol% were generally found to be completely immobile.

The immobility of lipid dyes entrained in films of adsorbed PEO-PBd amphiphiles has been attributed¹⁰ to the strong coupling between the polymer component and the substrate, creating barriers of immobile polymer in hybrid films. These barriers slow diffusion of the mobile film components and prevents diffusion entirely above the percolation threshold of the immobile polymer fraction.¹¹ The adsorption presumably stems from the interaction between the hydrogen bond donors

Table 1. Diffusion coefficients of labelled DHPE in DOPC/ $\text{EO}_{22}\text{Bd}_{37}$ hybrid lipid/polymer assemblies /films as a function of pH.

| $\text{EO}_{22}\text{Bd}_{37}$ mole % | A_{polymer}^a | pH 2 | pH 7 | pH 12 |
|--|------------------------|---|---|---|
| | | D ($\times 10^{-8} \text{ cm}^2/\text{s}$) | D ($\times 10^{-8} \text{ cm}^2/\text{s}$) | D ($\times 10^{-8} \text{ cm}^2/\text{s}$) |
| 0% | 0.00 | 1.8 ± 0.3 | 2.3 ± 0.2 | 3.8 ± 0.2 |
| 10% | 0.16 | 1.1 ± 0.2 | 1.55 ± 0.1 | 2.99 ± 0.03 |
| 25% | 0.37 | 0.26 ± 0.02 | 0.31 ± 0.01 | 0.68 ± 0.1 |
| 50% | 0.64 | -- | 0.06 ± 0.02^b | -- |
| 100% ^c | 1.00 | -- | -- | -- |

90% confidence intervals calculated using student t-scores for at least 3 measurements. ^a Fractional area of polymer in vesicles and films. ^b After incubating for 24 h at 40 $^{\circ}\text{C}$. ^c (99.4% with 0.6% TR-DHPE)

of the surface silanols present at silica interfaces and H-bond acceptors of the PEO block in the polymer. Indeed, clean silica presents a dense silanol surface capable of coupling – even multivalently – with the PEO block of the polymer chains.¹⁷ The protons of the surface silanols are pH labile ($\text{pK}_a \approx 7$),¹⁸ and the adsorption of PEO on silica has been shown to be a function of pH.¹⁷ These studies revealed that PEO does not generally adsorb on silica surfaces above pH 10, where the silanols are virtually all deprotonated.^{17b} More recent work reveals a narrow pH window for weak adsorption of PEO with lateral mobility on hydrophilic silica surfaces: below pH 7, strong adsorption of PEO is observed, while essentially no adsorption was observed above pH 8.8.¹⁹

We reasoned that the documented pH dependence of the PEO-silica interaction could be used to control the lateral fluidity of polymer and hybrid films adsorbed to glass cover slips. At high pH, silanols would be mostly deprotonated and significantly reduce the H-bond donating ability of the surface to the PEO in the amphiphilic polymers. To test this hypothesis, we measured the effective diffusion coefficients of TR-DHPE in hybrid and polymer films under acidic (pH 2) or basic (pH 12) conditions using FRAP methods (Table 1). Our results reveal that polymer and hybrid films on silica are not significantly more sensitive to changes in pH than the lipid only films. While the mobility in hybrid films was significantly faster under basic conditions than under acidic conditions (~ 2.6 – $2.7\times$ faster at pH 12), similar changes were observed for the DOPC-only bilayers ($\sim 2.1\times$ faster at pH 12). Furthermore, fluidity of hybrid films with higher polymer fractions (50 and 99.4 mol% with TR-DHPE) were insensitive to pH changes, and the lipid dye remained completely immobile even at elevated pH conditions.

In more heterogeneous films that consist of a high concentration of adsorbed but unfused vesicles (e.g. films with >50 mol% polymer), the discrete vesicles would not produce a coating that was continuous, which is required to facilitate fluorescence recovery via diffusion of the lipid dye from unbleached regions. More complete fusion could be facilitated by increasing the time and the temperature that the vesicle suspensions were incubated on the glass slides, resulting in more continuous hybrid lipid/polymer films. To test this hypothesis, we facilitated more complete vesicle fusion by incubating a clean glass cover slip with a suspension of vesicles with 50 mol% polymer for longer times (24 h) at elevated temperatures (40 °C). These hybrid films exhibited low but measurable mobility of the lipid dye, in contrast to the complete lack of mobility in identical coatings prepared at room temperature over 30 min. This result indicated that incomplete fusion may be at least partially responsible for the lack of fluidity in films with higher polymer compositions (>50 mol%).

To provide insight into the mechanism of adsorption and fusion of hybrid vesicles to silica surfaces, we monitored the formation of hybrid films using quartz crystal microbalance with dissipation (QCM-D, Figure 2), using a borosilicate glass coating over a gold QCM-D sensor as a proxy for the borosilicate glass cover slips. To prevent delamination of the sensor electrodes, RF plasma treatment in a reduced pressure atmosphere was used to clean the substrates rather than chemical etching. The interaction between DOPC vesicles and the silica substrate exhibited a typical QCM-D response: a rapid decrease in sensor frequency upon the adsorption of lipid vesicles, followed by a rapid but less pronounced increase in frequency that stabilized within 3 minutes to around $\Delta f = -25$ Hz. Along with the corresponding changes in energy dissipation ($\Delta D = 0.1 \times 10^{-6}$), these results indicated a continuous hydrated supported lipid bilayer.^{7a} The addition of vesicles containing 10 mol% EO₂₂Bd₃₇ also resulted in vesicle adsorption and fusion, but over much longer timescales (~15 min). Furthermore, the much more pronounced change in dissipation, ΔD , reflected a more viscoelastic response of the hybrid vesicles. These results indicate that even small amounts of added polymer dramatically affected the interaction of vesicles with the substrate as well as the viscoelastic properties of the film. At higher polymer fractions there was no distinction between the adsorption of vesicles and their fusion to the surface indicating that adsorption and any fusion that takes place are not separate, distinguishable events as in the case of pure lipid, even after 1.5 h (Figure S1). The gradual decrease in Δf and corresponding increase in ΔD suggest either adsorption without fusion of vesicles, or vesicle fusion that occurs on the same or much faster timescales as adsorption. At mole fractions below 50% polymer it is likely a combination of both effects – the adsorption and fusion of polymer-containing vesicles – based on our observations using confocal fluorescence and atomic force microscopies (Figure 1), which revealed both smooth surfaces

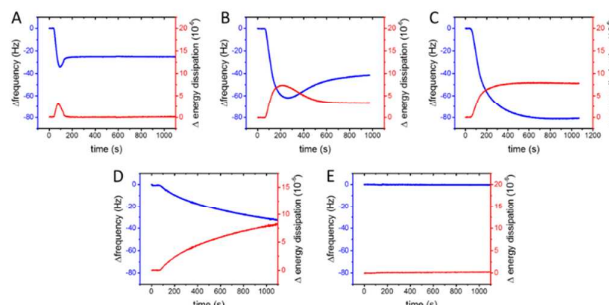


Figure 2 – Quartz crystal microbalance with dissipation (QCM-D) monitoring ($n=3$, i.e. 3rd overtone; see Figure S6 in the Electronic Supplementary Information for $n=3, 5, 7, 9$) of hybrid lipid/polymer film formation on plasma-cleaned borosilicate glass substrates. The baseline buffer measurement was stabilized and the vesicle solution (0.1 mg/mL) of either pure DOPC (A), 10 (B), 25 (C), 50 (D), and 100 (E) mol% of EO₂₂Bd₃₇ was injected.

at low polymer fractions as well many adsorbed vesicles at higher polymer fractions.

Considering the spectrum of outcomes with hybrid vesicle-silica interactions – from continuous bilayers to adsorbed vesicle films as the polymer fraction increased from 0 to 100 mol% – the results from QCM-D analysis were, for the most part, consistent with our analysis using confocal and atomic force microscopies. However, and quite unexpectedly, polymer-only vesicles (100 mol%) did not interact with the plasma-cleaned borosilicate substrates at all. Even over longer incubation times (1-2 h) or at elevated temperatures (40 °C), the frequency (Δf) and dissipation energy (ΔD) never changed more than about -0.5 Hz and 0.5×10^{-6} , respectively (Figure S2).

The variable interaction of polymer vesicles with cover glass seemed to depend on the cleaning treatment of the glass substrates. Importantly, the QCM-D sensors do not survive the chemical etching treatment that we used for confocal microscopy experiments, so we prepared some surfaces with plasma treatment. Using confocal microscopy, we found that polymer vesicles interacted substantially on glass cleaned using the chemical etching treatment (Figure 1). On the other hand, plasma-cleaned glass cover slips were unable to adsorb polymer vesicles. Suspensions of pure lipid and polymer vesicles that included ~1% TR-DHPE for imaging were incubated over plasma-cleaned glass, rinsed, and imaged by LCSM under identical conditions (Figure S3), and the average fluorescence intensity of the sample prepared from polymer vesicles was a mere 1% that of the lipid sample, which, in contrast, formed highly uniform lipid bilayers.

Based on a sampling of the literature, liquid-phase lipid bilayers may be formed on substrates treated with RF plasma,^{5, 20} acidic hydrogen peroxide,^{11, 20} or boiling detergent,²¹ and that these bilayers were mobile with similar lipid diffusion coefficients in the range of $1-8 \times 10^{-8}$ cm²/s, as first reported by Tamm and McConnell.^{1b} Our review of the literature suggests that differences in cleaning protocols among research groups reflect preferences based on convenience and compatibility with the experiments, and that in general these protocols can be used interchangeably to produce hydrophilic surfaces conducive to the formation of supported bilayers. However, our experiments indicate that in

contrast to DOPC vesicles, which seem to have no particular preference for the way the hydrophilic glass is prepared, 100 mol% PEO-PBd vesicles (or 99.4% with 0.6% TR-DHPE) do not interact significantly with plasma-treated glass surfaces.

The reasons for this difference between polymer vesicle interactions with chemically-etched and plasma-treated surfaces are not yet clear. We have analysed chemically-etched and plasma-cleaned surfaces by surface wettability measurements, X-ray photoelectron spectroscopy (XPS), and AFM surface roughness measurements (see Electronic Supplementary Information). Survey and high resolutions XPS scans of surfaces revealed small differences between chemically-etched and plasma-treated samples, which may account for the differences in polymer vesicle interaction. Specifically, relative to the chemically-etched sample, the plasma-treated sample shows elevated OH and Si-OH (see Table S2). In terms of surface roughness, only slight differences between samples cleaned in different ways were observed, but no significant differences that might account for the differences in polymer vesicle interaction. Surface roughness has been invoked to explain differences in lipid vesicle interaction with surfaces,²² but those differences were not observed by us for lipid bilayers, and it is still not clear how roughness differences prevent or otherwise affect the interaction of the 100 mol% polymer vesicles (or 99.4 mol% with TR-DHPE). Nevertheless, it is important to point out that special care and attention may be needed when preparing substrates for the formation of supported hybrid lipid/polymer films.

The properties of the hybrid films can be interrogated by modelling and analysing the QCM-D data. The adsorption onto a resonating sensor results in a change in the sensor's resonant frequency, Δf , that is proportional to the mass of the adsorbed materials described by Sauerbrey.²³ The so-called Sauerbrey model was found to be valid for rigid and semi-rigid films provided the energy dissipation, ΔD , is less than 2×10^{-6} .²⁴ We monitored Δf and ΔD at different harmonics ($n=3,5,7,9$) to follow the interaction of hybrid lipid/polymer vesicles with silica surfaces. The different responses observed at the different harmonics and the substantial dissipation (Figure 2, see also Electronic Supplementary Information Figure S6) are consistent with the adsorption of viscoelastic materials observed previously,^{7b, 25} indicating that the hybrid lipid/polymer films that assemble on glass surfaces, even with as little as 10 mol% PEO-PBd, have viscous and elastic properties different from 100 mol% lipid bilayers.

These adsorbed materials were analysed using the Voigt-Voinova model.²⁶ This model treats the adsorbed film as a continuous layer that acts as Voigt element with a shear viscosity and a shear modulus. As a result, this treatment can be used to estimate thickness, viscosity, and shear modulus of the adsorbed layers at the end of the 15 min QCM-D experiments, assuming a solution viscosity of $0.001 \text{ N}\cdot\text{s}/\text{m}^2$ and the density of the adsorbed lipid/polymer material as $1 \text{ g}/\text{cm}^3$ (Table 2). DOPC bilayers had measured a bilayer thickness and areal mass comparable to previous examples of supported lipid bilayers.²⁷ On the other hand, calculated X^2 values of the model fit were significantly higher,

indicating that the standard Voigt-Voinova model may not be appropriate to describe for the adsorption of materials with increasing polymer content. Richter et al. raised concerns about the use of this model to describe the adsorption heterogeneous films.²⁸ Furthermore, the Voigt-Voinova assumes the viscosity and the shear modulus are frequency independent. This

Table 2. Hybrid lipid/polymer assembly properties extracted from Voigt-Voinova model of QCM-D data^a

| | thickness (nm) | areal mass (ng/cm ²) | viscosity ($\times 10^{-3} \text{ N}\cdot\text{s}/\text{m}^2$) | shear modulus ($\times 10^4 \text{ N}/\text{m}^2$) | X^2 ($\times 10^4$) ^d |
|-------------------|----------------------|----------------------------------|--|--|--------------------------------------|
| 0% | 5.3±0.2 | 530±20 | 4.8±0.7 | b | 7 |
| 10% | 8.06±0.05 | 806±5 | 3.4±0.2 | 3.8±0.1 | 123 |
| 25% | 15.33±0.04 | 1533±4 | 2.78±0.01 | 3.91±0.04 | 239 |
| 50% | 7.6±0.1 ^c | 760±10 | 1.41±0.04 | 1.41±0.02 | 22 |
| 100% ^e | e | e | e | e | e |

^a Model fit using Δf and ΔD data from 4 overtones ($n=3,5,7,9$) taken over 16 minutes (2380 time points), with averages (\pm standard error of mean) obtained between 800–900 s. ^b Shear modulus for films prepared from DOPC varied significantly around zero and a reliable average could not be obtained. ^c Not a stable steady-state value, as the surface continuously adsorbs material up to at least 90 minutes (see Figure S1). ^d Chi-square for the model fit. ^e No vesicle adsorption or fusion observed for 100% polymer vesicles (see Figure S1).

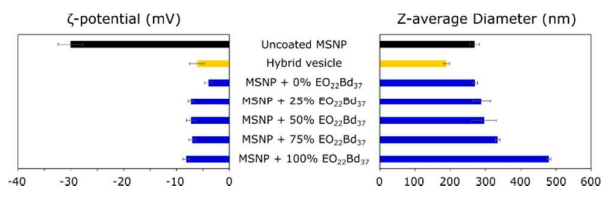


Figure 3. Zeta potential measurements from DLS (left) and z-average diameter measurements from DLS (right) for uncoated MSNPs, hybrid vesicles (the average for vesicles comprised of 0, 25, 50, 75, and 100 mol%), and MSNPs coated with DOPC (0% EO₂₂Bd₃₇), and hybrid membranes comprised of DOPC and 25, 50, 75, and 100 mol% EO₂₂Bd₃₇. Units are mV (left) and nm (right). Error bars represent standard error of the mean for $n=3$ measurements.

assumption may not valid for adsorbed layers containing PEO-PBd, yet these hybrid lipid/polymer systems offer an intriguing model system that spans the transition from rigid supported bilayers to increasingly viscoelastic films.

Fusion to Silica Particles. Coated particles have received significant attention as drug delivery vehicles.⁴ Our observations of hybrid lipid/polymer films on 2D silica surfaces was born out on 3D silica surfaces as well, and mirrored those of the planar surfaces described above. MSNPs were used in lieu of borosilicate cover glass. Incubating hybrid vesicles with MSNPs in 0.5x PBS produced stable suspensions of coated particles. Zeta potential analysis revealed that the highly negative MSNPs, $\zeta = -30 \text{ mV}$, were efficiently coated with hybrid membrane material that increased the potential of the resulting structures closer to that of the hybrid vesicles, $\zeta = -7$ to -8 mV (Figure 3). DLS analysis demonstrated the size distribution remained stable with the addition of the hybrid coatings, indicating a lack of aggregation except in the case of 75 and 100 mol% polymer coatings.

Conformal hybrid coatings were confirmed by cryo-EM (Figure 4) after incubation of MSNPs with 10, 25, 50, and 75

mol% EO₂₂Bd₃₇. While structure of hybrid lipid/polymer films on 2D surfaces was somewhat ambiguous, cryo-EM imaging revealed that these hybrid materials formed conformal layers at MSNP interfaces were 8-10 nm thick. These thicknesses are comparable to vesicle bilayer thicknesses^{13c} and consistent with bilayer coatings. In addition to hybrid lipid/polymer coatings, we also observed some adsorbed and unfused vesicles in the MSNP sample containing 75 mol%. No conformal bilayer coatings were observed for 100 mol% polymer vesicles incubated with MSNPs. The decreased propensity of hybrid vesicles to fuse as the polymer content increased stems from the enhanced mechanical properties of polymer vesicles. Discher et al. related²⁹ vesicle “toughness” to measured cohesive energy densities, E_c , and found that polymeric membranes similar to the ones reported here were 5-50 times tougher than natural phospholipid membranes. A natural consequence of the higher cohesive energy density is a higher energy barrier required to rupture polymer vesicle membranes that allow their fusion to solid supports. Hybrid vesicles with intermediate polymer compositions, and presumably intermediate cohesive energy densities, demonstrate a corresponding propensity to form supported bilayers over

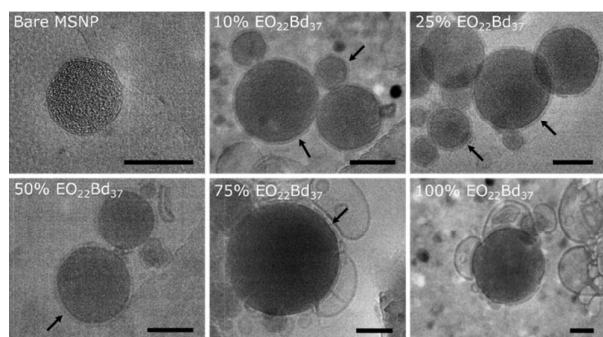


Figure 4 –Cryo-EM images of bare MSNP and MSNPs in the presence of hybrid membranes comprised of DOPC and 10, 25, 50, 75, and 100 mol% EO₂₂Bd₃₇. Arrows indicate presence of bilayer coatings on particles. Hybrid membranes with higher polymer fractions (75 and 100 %) also resulted in adsorbed vesicles (Scale bar = 100 nm)

mesoporous silica. These results mirror our observations of hybrid vesicle interaction with 2D cover glass supports discussed above.

Conclusions

We have demonstrated that hybrid vesicles – comprised of the fluid-phase lipid DOPC and amphiphilic poly(ethylene oxide-*b*-butadiene) – adsorb and fuse not only to planar silica substrates, but also porous spherical silica particles as well. Confocal fluorescence and atomic force microscopies revealed that adsorption, rather than fusion, is preferred for vesicles with higher fractions (>50 mol%) of polymer EO₂₁Bd₃₇. In addition, the lateral fluidity of the adsorbed films decreased as the fraction of polymer increased, with 100% poly(ethylene

oxide-*b*-butadiene) (99.4 mol% with TR-DHPE) exhibiting no mobility. While the mobility in all supported lipid/polymer films we tested increased with pH, the observed fluidity of hybrid films was found to be just as sensitive to changes in pH as pure lipid bilayers. Quartz crystal microbalance with dissipation measurements revealed that the polymer slowed the adsorption and fusion processes with silica, and that RF plasma cleaning treatments significantly reduced the interaction between pure polymersomes and silica. Nevertheless, conformal hybrid lipid/polymer bilayer coatings could be formed on mesoporous silica nanoparticles and imaged via cryo-electron microscopy. These results expand the library of materials that can be used for coating silica-based nanoparticles, and may also improve the stability of the resulting hybrid lipid/polymer films relative to lipid-based bilayer films.

Conflicts of interest

The authors declare no conflicts of interest.

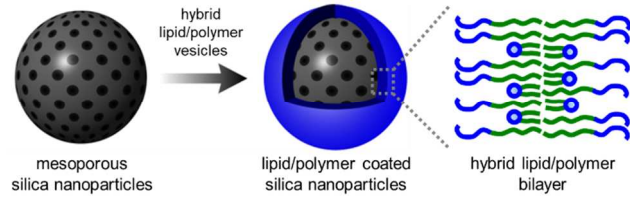
Acknowledgements

This work was performed in part, at the Center for Integrated Nanotechnologies, an Office of Science User Facility operated for the U.S. Department of Energy (DOE) Office of Science (project number 2017BC0053). Research was supported by the Laboratory Directed Research and Development program at Sandia National Laboratories, a multi-mission laboratory managed and operated by National Technology and Engineering Solutions of Sandia, LLC, a wholly owned subsidiary of Honeywell International, Inc., for the U.S. Department of Energy's National Nuclear Security Administration under contract DE-NA-0003525.

Notes and references

- (a) Sackmann, E. *Science* **1996**, *271*, 43-48. (b) Tamm, L. K.; McConnell, H. M. *Biophysical Journal* **1985**, *47*, 105-113.
- Dustin, M. L.; Groves, J. T., Receptor signaling clusters in the immune synapse. In *Annual review of biophysics*, vol 41, Rees, D. C., Ed. Annual Reviews: Palo Alto: 2012; Vol. 41, pp 543-556.
- (a) Bally, M.; Bailey, K.; Sugihara, K.; Grieshaber, D.; Voros, J.; Stadler, B. *Small* **2010**, *6*, 2481-2497. (b) Martinez, J. A.; Misra, N.; Wang, Y.; Stroeve, P.; Grigoropoulos, C. P.; Noy, A. *Nano Letters* **2009**, *9*, 1121-1126. (c) Misra, N.; Martinez, J. A.; Huang, S.-C. J.; Wang, Y.; Stroeve, P.; Grigoropoulos, C. P.; Noy, A. *Proceedings of the National Academy of Sciences of the United States of America* **2009**, *106*, 13780-13784.
- (a) Durfee, P. N.; Lin, Y. S.; Dunphy, D. R.; Muniz, A. J.; Butler, K. S.; Humphrey, K. R.; Lokke, A. J.; Agola, J. O.; Chou, S. S.; Chen, I. M.; Wharton, W.; Townson, J. L.; Willman, C. L.; Brinker, C. J. *ACS Nano* **2016**, *10*, 8325-8345. (b) Liu, J. W.; Stace-Naughton, A.; Jiang, X. M.; Brinker, C. J. *J. Am. Chem. Soc.* **2009**, *131*, 1354+. (c) Yao, V. J.; D'Angelo, S.; Butler, K. S.; Theron, C.; Smith, T. L.; Marchio, S.; Gelovani, J. G.; Sidman, R. L.; Dobroff, A. S.; Brinker, C. J.; Bradbury, A. R. M.; Arap, W.; Pasqualini, R. *Journal of Controlled Release* **2016**, *240*, 267-286.

5. Kalb, E.; Frey, S.; Tamm, L. K. *Biochimica et Biophysica Acta (BBA) - Biomembranes* **1992**, *1103*, 307-316.
6. (a) Mornet, S.; Lambert, O.; Duguet, E.; Brisson, A. *Nano Letters* **2005**, *5*, 281-285. (b) Liu, J.; Jiang, X.; Ashley, C.; Brinker, C. J. *J. Am. Chem. Soc.* **2009**, *131*, 7567-7569.
7. (a) Keller, C. A.; Kasemo, B. *Biophysical Journal* **1998**, *75*, 1397-1402. (b) Reimhult, E.; Hook, F.; Kasemo, B. *Langmuir* **2003**, *19*, 1681-1691.
8. (a) Zhdanov, V. P.; Dimitrievski, K.; Kasemo, B. *Langmuir* **2006**, *22*, 3477-3480. (b) Dimitrievski, K.; Kasemo, B. *Langmuir* **2008**, *24*, 4077-4091.
9. Richter, R. P.; Berat, R.; Brisson, A. R. *Langmuir* **2006**, *22*, 3497-3505.
10. Goertz, M. P.; Marks, L. E.; Montañó, G. A. *ACS Nano* **2012**, *6*, 1532-1540.
11. Gettel, D. L.; Sanborn, J.; Patel, M. A.; de Hoog, H.-P.; Liedberg, B.; Nallani, M.; Parikh, A. N. *J. Am. Chem. Soc.* **2014**, *136*, 10186-10189.
12. Hamai, C.; Yang, T. L.; Kataoka, S.; Cremer, P. S.; Musser, S. M. *Biophysical Journal* **2006**, *90*, 1241-1248.
13. (a) Nam, J.; Beales, P. A.; Vanderlick, T. K. *Langmuir* **2011**, *27*, 1-6. (b) Khan, S.; Li, M.; Muench, S. P.; Jeuken, L. J. C.; Beales, P. A. *Chem. Commun.* **2016**, *52*, 11020-11023. (c) Paxton, W. F.; McAninch, P. T.; Achyuthan, K. E.; Shin, S. H. R.; Monteith, H. L. *Colloids and Surfaces B: Biointerfaces* **2017**, *159*, 268-276. (d) Schulz, M.; Binder, W. H. *Macromolecular Rapid Communications* **2015**, *36*, 2031-2041. (e) Schulz, M.; Glatte, D.; Meister, A.; Scholtyssek, P.; Kerth, A.; Blume, A.; Bacia, K.; Binder, W. H. *Soft Matter* **2011**, *7*, 8100-8110.
14. Lu, Y. F.; Fan, H. Y.; Stump, A.; Ward, T. L.; Rieker, T.; Brinker, C. J. *Nature* **1999**, *398*, 223-226.
15. Blumenthal, D.; Goldstien, L.; Eddin, M.; Gheber, L. A. *Sci Rep* **2015**, *5*, 9.
16. Schneider, C. A.; Rasband, W. S.; Eliceiri, K. W. *Nat. Methods* **2012**, *9*, 671-675.
17. (a) Stuart, M. A. C.; Tamai, H. *Langmuir* **1988**, *4*, 1184-1188. (b) Rubio, J.; Kitchener, J. A. *Journal of Colloid and Interface Science* **1976**, *57*, 132-142. (c) Joppien, G. R. *The Journal of Physical Chemistry* **1978**, *82*, 2210-2215. (d) Malmsten, M.; Linse, P.; Cosgrove, T. *Macromolecules* **1992**, *25*, 2474-2481. (e) Killmann, E.; Maier, H.; Baker, J. A. *Colloids and Surfaces* **1988**, *31*, 51-71. (f) Cosgrove, T. *J. Chem. Soc.-Faraday Trans.* **1990**, *86*, 1323-1332. (g) Vanderbeek, G. P.; Stuart, M. A. C.; Cosgrove, T. *Langmuir* **1991**, *7*, 327-334. (h) Killmann, E.; Maier, H.; Kaniut, P.; Gutling, N. *Colloids and Surfaces* **1985**, *15*, 261-276. (i) Char, K.; Frank, C. W.; Gast, A. P. *Langmuir* **1990**, *6*, 767-770. (j) Char, K.; Gast, A. P.; Frank, C. W. *Langmuir* **1988**, *4*, 989-998.
18. Hiemstra, T.; De Wit, J. C. M.; Van Riemsdijk, W. H. *Journal of Colloid and Interface Science* **1989**, *133*, 105-117.
19. Yu, C.; Guan, J.; Chen, K.; Bae, S. C.; Granick, S. *ACS Nano* **2013**, *7*, 9735-9742.
20. Groves, J. T.; Ulman, N.; Boxer, S. G. *Science* **1997**, *275*, 651-653.
21. (a) Hamai, C.; Cremer, P. S.; Musser, S. M. *Biophysical Journal* **2007**, *92*, 1988-1999. (b) Hamai, C.; Yang, T.; Kataoka, S.; Cremer, P. S.; Musser, S. M. *Biophysical Journal* **2006**, *90*, 1241-1248.
22. Kumar, A.; Dahl, V.; Kleinen, J.; Gambaryan-Roisman, T.; Venzmer, J. *Colloids and Surfaces A: Physicochemical and Engineering Aspects* **2017**, *521*, 302-311.
23. Sauerbrey, G. *Zeitschrift für Physik* **1959**, *155*, 206-222.
24. White, C. C.; Schrag, J. L. *The Journal of Chemical Physics* **1999**, *111*, 11192-11206.
25. Höök, F.; Kasemo, B.; Nylander, T.; Fant, C.; Sott, K.; Elwing, H. *Anal. Chem.* **2001**, *73*, 5796-5804.
26. Voinova, M. V.; Rodahl, M.; Jonson, M.; Kasemo, B. *Phys. Scr.* **1999**, *59*, 391-396.
27. (a) Cho, N.-J.; Kanazawa, K. K.; Glenn, J. S.; Frank, C. W. *Anal. Chem.* **2007**, *79*, 7027-7035. (b) Keller, C. A.; Glasmästar, K.; Zhdanov, V. P.; Kasemo, B. *Physical Review Letters* **2000**, *84*, 5443-5446.
28. Reviakine, I.; Johannsmann, D.; Richter, R. P. *Anal. Chem.* **2011**, *83*, 8838-8848.
29. Discher, B. M.; Won, Y. Y.; Ege, D. S.; Lee, J. C. M.; Bates, F. S.; Discher, D. E.; Hammer, D. A. *Science* **1999**, *284*, 1143-1146.



We monitored the interaction of hybrid lipid/polymer vesicles with planar and spherical silica substrates via confocal microscopy, AFM, QCM-D, and cryo-EM.